Available online at www.sciencedirect.com
SCIENCE DIRECT®
Catalysis Today 107–108 (2005) 192–199
CATALYSIS TODAY
www.elsevier.com/locate/cattod

PILC-based monolithic catalysts for the selective catalytic reduction of nitrogen oxides by methane in oxygen excess

F. Mohino, P. Avila, P. Salerno, A. Bahamonde, S. Mendioroz *

Instituto de Catálisis y Petroleoquímica, CSIC, C/Marie Curie No. 2, 28049 Madrid, Spain

Abstract

The aim of this work was the study and development of aluminum-pillared clay (Al-PILC)-based monolithic Pd catalysts for reducing NO_x emissions from natural gas-fired power plants using methane as a selective reductant. During preparation of the support, the same raw material used to synthesize the pillared clays was used as a permanent inorganic binder. This confers high surface area and acidity to the extrudates, in addition to high hydrothermal resistance and mechanical strength. The influence of the method used for active phase incorporation on the physico-chemical properties and $DeNO_x$ activity and selectivity was studied. Conclusions were drawn from the use of different solution pH values and precursors in relation to the isoelectric point of the solid. Characterization was carried out using X-ray diffraction, inductively coupled plasma-optical emission spectroscopy, X-ray photoelectron spectroscopy, N_2 adsorption, and NH_3 and CO chemisorption.

Keywords: Al-PILC; Pd catalysts; Monolithic supports; $DeNO_x$; CH_4

1. Introduction

Selective catalytic reduction (SCR) is a well-established process for NO_x removal from power plant emissions. This process consists of the reduction of nitrogen oxides (typically 95% nitric oxide) to innocuous water and nitrogen, by means of ammonia (either as a gas or in aqueous solution) as the reducing agent. However, at present, there is a great incentive to use natural gas or other hydrocarbons as the reductant in stationary SCR units rather than NH_3 for the following reasons. Firstly, in many new power plants, natural gas is commonly used as the fuel and is thus readily available. Secondly, ammonia is more expensive, requires special handling and storage, and needs a sophisticated metering system to avoid NH_3 slip. The main advantage of the reaction between nitric oxide and hydrocarbons in post-combustion processes is the use of a gas mixture similar to that found in the exhaust. Given the plentiful supply of natural gas worldwide, its use as a selective reductant makes it a desirable option for NO_x emission control, due to the benefits of low cost compared to other hydrocarbons and much lower corrosiveness than ammonia.

Different catalytic supports based on metal oxides, such as alumina, zirconia and titania among others [1,2], have traditionally been used in NO_x SCR with hydrocarbons. More recently, zeolites, either acidic or not and interchanged or not with transition metals, have shown high efficiency in this process [3,4]. Although metal-exchanged zeolite catalysts generally exhibit high activity for this reaction, most of these metastable structures suffer from deactivation problems when exposed to wet exhaust streams at elevated temperatures, and thus more stable structures are being sought [5]. With this objective, pillared clays are being introduced due to their tunable acidity and porosity [6].

In recent years, pillared clays (PILCs) have been used as catalyst supports in an increasing number of processes because of their textural and acidic properties [7], including some air pollution control processes [8–12]. Among these, $DeNO_x$ processes are especially relevant: Rh-impregnated

---

* Corresponding author. Fax: +34 915855475.
E-mail addresses: abahamonde@icp.csic.es (A. Bahamonde), sme@icp.csic.es (S. Mendioroz).

0920-5861/$ – see front matter © 2005 Published by Elsevier B.V.
doi:10.1016/j.cattod.2005.07.090

AZA and FAZA used in the reduction of NO by CO [13,14]; Cr–Fe/Ti-PILC [15] and Fe/Ti–H^+-PILC [16] in NO SCR by NH_3; Cu^{2+} ion-exchanged Al-, Ti- and Zr-pillared clays [17]; and Cu, Fe, Ce, Co, Ag, Ga and Ce-promoted Cu-exchanged Ti-PILC [6] in NO SCR by ethylene. In general, these pillared structures are not as sensitive as zeolites to the presence of water vapor and SO_2.

Pillared clays are two-dimensional zeolite-like materials. They are prepared by exchanging the charge compensating cations within the clay with large inorganic hydroxycations formed by hydrolysis of metal oxides or salts. Upon heating, the cations undergo dehydration and dehydroxylation and form stable metal oxide clusters, which act as pillars between adjacent layers and thus form stable porous structures. Their pore size depends on the oligocation charge, the number of exchangeable cations of the clay and the extent of the exchange [18].

Structured monolithic catalysts are widely used for end-of-pipe processes. They have been found to be effective in the cleaning of exhaust gases from stationary and mobile sources because they offer very low pressure drop, high resistance to plugging, and high geometric area per unit volume, which make them very useful in solid-catalyzed gas-phase chemical reactions [19,20]. They are extensively used in automotive [19] and stationary emission control [21], but they are also increasingly used in many other applications, such as in chemical processing industries, catalytic combustion [22], pollution abatement of volatile organic chemicals, and oxidation of carbon monoxide and unburned hydrocarbons, among others [23]. By 1975, production model automobiles were equipped with monolithic catalytic converters. In 1985, approximately 100 million catalytic units were in use in the United States alone. At present, several hundred million converters are in everyday operation, mostly in the United States and Europe [19]. The use of catalysts for auto-exhaust emission control represents one of the largest single catalyst uses.

The last step in the process of preparing a monolith-supported catalyst involves incorporating the active material. Catalytically active ingredients must be uniformly dispersed over the whole porous monolithic surface, and their incorporation adds an additional variable to the final structure.

Adsorption of metals from precursor salt solutions is often used to prepare dispersed metal catalysts [24,25]. Properties such as acidity, metallic dispersion, metal–support interaction and reactivity are dependent on the pH of the impregnating solution in relation to the state of the support surface [26].

The adsorption of metals on alumina [27–29] has been intensely studied in the past, but details of the adsorption processes involved in the preparation are still unclear. Among the earlier works aimed at scientifically describing metal complex adsorption is the seminal paper by Brunelle [30]. At present there is no information on adsorption by pillared clays, probably because the number of factors that can alter the clay hydrous surface. These include: loss of water, from either the external surface or the interlayer, hydrolysis of CUS or the hydrous alumina forming the pillar, the presence of different exchangeable cations with different exchange equilibrium, etc., which depend on the pH, making the process difficult to understand. The development of charges on the clay surface and hence the possibility of metal adsorption is dependent on the pH of the solution in which it is immersed. In its turn, the metallic species in solution can also acquire different chemical states, depending on the pH. Concerning palladium ions, they form various complexes with chloride and/or ammonium ligands at room temperature, with electric charges between −2 and +2, although, in general, the chemical state of palladium ions in aqueous solutions depends on the pH and on other solution variables, such as concentration or temperature [31]. As a consequence, metal impregnation cannot be visualized as a straightforward process. The overall adsorption equilibrium depends on the electrical charge of the complex species and their reactivity, and on the clay surface state, both of which are affected by the solution pH.

This paper is concerned not only with the possibility of using pillared clays as high-surface-area supports for Pd-based catalysts, but also with a study of the influence of the solution impregnating pH on the physico-chemical properties of the final catalysts and their activity and selectivity in the NO_x SRC by methane in oxygen excess.

2. Experimental

2.1. Characterization methods

Chemical analyses were carried out on a Perkin-Elmer Optima 3300 DV spectrometer using the inductively coupled plasma-optical emission spectroscopy (ICP-OES) on acid-dissolved samples. X-ray diffraction (XRD) patterns were recorded with a Seifert XRD300 diffractometer using Ni-filtered Cu Kα radiation in the 2θ range 3–30°.

Nitrogen adsorption–desorption isotherms were determined on a TriStar Micromeritics instrument at 76 K after outgassing the samples overnight at 350 °C. The specific surface area was calculated using the BET treatment taking 0.162 nm^2 for the cross-sectional area of an adsorbed N_2 molecule. Micro- and meso-porosity were determined by application of the *t*-plot and the BJH methods, respectively, to the isotherm data. Porosity studies were completed by mercury intrusion porosimetry using CE Instruments Pascal 140/240 apparatus and applying the Washburn equation for cylindrical pores with the IUPAC recommended values of 141° and 484 mN/m, respectively, for the contact angle and surface tension of mercury. The total pore volume (V_{total}) was evaluated by combining both of these techniques.

Ammonia adsorption at room temperature measured on an ASAP-2010C instrument (Micromeritics) was used to evaluate acidity. After outgassing for 2 h at 350 °C, the sample was exposed to increasing ammonia pressures in the relative pressure range 0.01–0.25 at room temperature. A second adsorption (physisorption) process after outgassing the sample at room temperature for 4 h gives the amount of chemisorbed ammonia by difference from the previous run. This was used to evaluate the total number of acidic centers expressed as meq NH_3/g sample.

CO chemisorption was also determined on an ASAP 2010C instrument for samples outgassed at 350 °C and reduced in flowing H_2 at the same temperature for 4 h. Evaluation of the metallic dispersion was made considering a stoichiometry for CO chemisorption on Pd of 1.15:1.

X-ray photoelectron spectra (XPS) were obtained using a Fisons Escalab 200R spectrometer with a hemispherical analyzer operating in the constant-pass energy mode. Non-monochromatized Mg Kα X-ray radiation at 10 mA and 12 kV was used as the exciting source. The Al 2p line at binding energy of 74.5 eV was used as the internal standard. The atomic ratios of the surface elements were estimated from the integrated intensities of Pd $3d_{5/2}$, Si 2p and Al 2p peaks using the Wagner sensitivity factors.

The axial crushing strength of the monoliths was measured using a constant-loading-rate Chatillon Model LTCM Universal Tensile and Spring tester with a 1-mm^2 test head.

2.2. Catalytic activity

Catalytic activity tests were carried out in an integral monolithic reactor under PC control. A scheme of the experimental set-up is depicted in Fig. 1. Dead space between the honeycomb catalyst and the reactor wall was filled with an inert material to prevent gas by-pass. All the lines were heated to avoid possible water condensation.

The operating conditions were: temperature range, 350–500 °C; total gas flow, 3600 N cm^3/min; gas hourly space velocity (GHSV), 3600 h^{-1}; and V_{linear}, 0.4 mN s^{-1}. Inlet concentrations were as follows: [CH_4], 5000 ppm; [NO], 500 ppm; [O_2], 1.2 vol.%; and N_2 to balance. Continuous inlet and outlet contents were quantified using a SIGNAL 4000 VM chemiluminescence NO/NO_x analyzer for NO_x, a HORIBA FIA-510 flame-ionization detector analyzer for CH_4, and a HORIBA VIA-510 non-dispersive infrared analyzer for CO_2.

2.3. Catalyst preparation

2.3.1. Starting material

The parent clay was a montmorillonite from Cabañas, Toledo, Spain, provided by TOLSA S.A. This was a trioctahedral, high-purity (98% phyllosilicates) smectite (subgroup saponite), with Ca, Mg and Na as the main exchangeable cations. The percentage chemical composition reported by the supplier was: 55.1% SiO_2, 6.46% Al_2O_3, 25.18% MgO, 0.58% CaO, 2.07% Fe_2O_3, 0.26% Na_2O, 0.78% K_2O, 0.20% Mn_2O_3, and <0.4 TiO_2, with 8.84% loss on ignition at 1000 °C. Its main physico-chemical properties were: specific surface area (S_{BET}), 132 m^2/g; total pore volume (V_{total}), 0.848 cm^3 g^{-1}; acidity (measured by NH_3 adsorption at room temperature), 0.72 meq NH_3/g; and cation exchange capacity (CEC), 74 meq/100 g. The Al-pillared clay (Al-PILC) prepared from this clay was used to support the Pd-based catalysts used in this work.

2.3.2. Pillaring procedure

Pillaring was achieved on the as-received montmorillonite dispersed in acetone (50 wt.%) and stirred for 24 h [32]. Measured volumes of pillaring solution (50% Locron®, an Al keggin cation marketed by Hoescht) in water were slowly

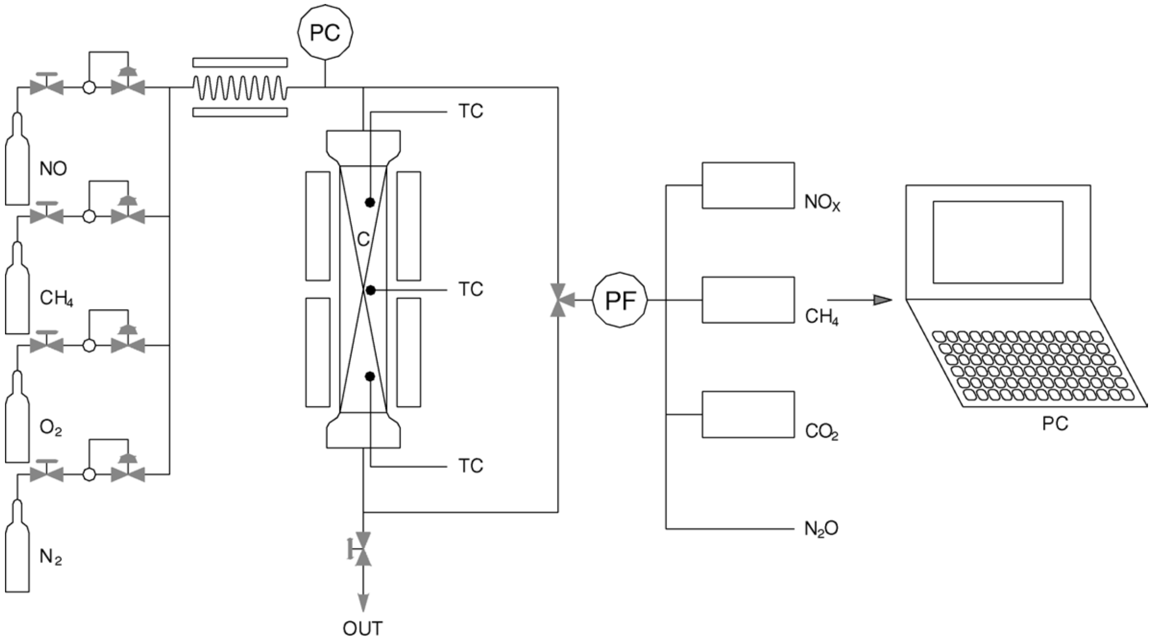

Fig. 1. Schematic diagram of the experimental system for DeNO$_x$ activity studies.

Table 1
Catalysts preparation conditions

Catalyst	Pd (wt.%)	Precursor salt	$pH_{initial}$	pH_{final}
C25	0.60	Pd $(OAc)_2$	4.30	4.64
C12	0.49	Pd Cl_2*	8.11	8.43
C13	0.24	Pd Cl_2*	9.00	9.47
C23	0.34	Pd $(OAc)_2$*	9.50	9.70

* Aqueous ammonia was added to form the corresponding ammine compound.

added to the mineral suspension with continuous stirring to achieve 20 meq Al/g clay; stirring was maintained for one additional hour. After removal of the solution, the suspensions were dialyzed against distilled water until anion-free (50 mS). Finally, the solids were dried at 80 °C and calcined at 500 °C for 2 h.

2.3.3. Preparation of the monolithic carrier

The monolithic supports used for preparing the Pd catalysts were manufactured from the previously synthesized Al-pillared clay as the main constituent. To a homogeneous mixture of Al-PILC and the as-received parent material used as binder at a weight ratio of 80/20, water was added to achieve a final solid/liquid relation of approximately 0.52 [33]. The particle size of the solids prior to mixing and kneading was <0.23 mm. After mixing and kneading of the components, the paste was extruded through a die, carefully dried at room temperature for 48 h, and finally calcined at 500 °C for 4 h. The monolith had square channels of 2.5-mm pitch with a wall thickness of 0.9 mm, cell density of 8.9 cell cm^{-2} and geometric surface area of 849 $m^2\ m^{-3}$. The axial crushing strength of the monolith was 180 kg cm^{-2}, high enough for use in industrial $DeNO_x$ processes [34].

2.3.4. Active phase incorporation

The active phase was incorporated using a variation of the incipient wetness impregnation method using specially designed equipment to achieve homogeneous impregnation. Aqueous salt solutions of palladium acetate or palladium chloride of adequate concentrations to obtain Pd contents from 0.2 to 0.6 wt.% were used to prepare the catalysts. Taking into account that the Al-PILC isoelectric point (IEP) was 2.8, aqueous ammonia solution was added to the chloride solutions to vary the pH in the interval 2.7–9.5 and thus facilitate metal incorporation as ammine complexes. Four Pd/Al-PILC catalysts were prepared from different precursor salts and pH values. Once the active phase was incorporated, the monoliths were dried in air for 12 h, then at 60 °C for 12 h, and finally calcined at 500 °C for 2 h in an air atmosphere. In Table 1 the preparation conditions for the complete series and the active phase contents are collated.

3. Results and discussion

The main physico-chemical properties of the parent raw material, Al-PILC, and the monolithic support (M500) are included in Table 2. Successful pillaring was accomplished after calcination of the exchanged clay at 500 °C, because permanent expansion of the basal spacing and an important increase in the specific surface area and porosity were detected in the resulting Al-PILC. It can also be appreciated that the properties of the monolith obtained (M500), surface area, micro- and meso-porosity, remained practically unchanged with respect to the Al-PILC. In contrast, macro-porosity was dramatically reduced as a consequence of paste compaction during the extrusion step.

The main physico-chemical properties of all catalysts studied are given in Table 3. No important variations in basal spacing or the textural properties were found in the dried and calcined catalysts compared to the monolithic support. This indicates the stability of the support at different pH values and thermal treatments up to 500 °C, and confirms the possibility of using pillared materials as catalyst supports of high surface area [33]. In contrast, some small differences in acidity with respect to the support and, much more importantly, in metallic dispersion among catalysts were observed for the catalysts compared to the support.

As previously stated, all changes in acidity and metallic dispersion in the catalysts are due not only to the surface charge of the solid, but also to the metallic species in solution and its electric charge, all of which are related to the IEP of the solid and the impregnating solution pH. It can be concluded that active phase incorporation to the Al-PILC-based monolithic support is governed by the following parameters.

3.1. The charge properties of the layer edges

Clays and pillared clays have in their constitution a significant amount of hydroxyls. In contact with the active phase solution, these hydroxyls may undergo either protonation (provided the impregnating solution pH is below the IEP of the solid) or deprotonation (pH > IEP of the solid), causing the solid surface to become positively or

Table 2
Physico-chemical properties of raw material, Al-PILC clay material and Al-PILC based monolithic support

Sample	d_{001} (Å)	CEC* (meq/100 g)	V_{micro} ($cm^3\ g^{-1}$)	V_{meso} ($cm^3\ g^{-1}$)	V_{macro} ($cm^3\ g^{-1}$)	S_{BET} (m^2/g)
Clay	14.3	74.0	0.020	0.090	0.720	132
Al-PILC	18.8	15.3	0.070	0.090	0.600	234
M500	18.2	–	0.045	0.083	0.330	223

* CEC: cation exchange capacity.

negatively charged and thus acting as anion or cation exchangers, respectively [35]

$$M{-}OH + H_3O^+ \leftrightarrow M{-}OH_2^+ + H_2O \quad (1)$$

$$M{-}OH + OH^- \leftrightarrow M{-}O^- + H_2O \quad (2)$$

Since Pd impregnation in most cases was carried out at pH values above the IEP of the solid [2,8], the solid surface would undergo deprotonation, and consequently would be negatively charged.

3.2. The speciation of the complex prevailing in solution and its electric charge

In this case the variables are the concentrations of H^+, Cl^- and NH_4^+, which can give rise to different anionic or cationic species following:

$$[Pd(NH_3)_{4-n}Cl_n]^{(2-n)+} + NH_4^+ \leftrightarrow Pd(NH_3)_{5-n}Cl_{n-1}]^{(3-n)+} + Cl^- + H^+, \quad (1 \le n \le 4) \quad (3)$$

with a coordination sphere consisting of ammonia or Cl^-, depending on the pH [31].

3.3. The adsorption equilibrium constant of the various species in solution

Each species formed has the possibility of adsorbing at the solid–liquid interphase, with this possibility being governed by the respective adsorption constants.

Besides, the adsorption of active species is usually accompanied by a series of secondary reactions, such as proton transfer in the interface, complex reaction in the bulk solution, interference among competitive species, etc. [36]. Here, two cationic phases are present in solution, corresponding, respectively to the dissolved metallic phase, whatever the complex formed, and protons, in a quantity depending again on the solution pH. Both of these will adsorb on the solid, depending on their respective equilibrium constants and concentrations. Thus, besides the metal, the solid will adsorb an additional amount of protons directly related to the proton concentration in the starting solution. In Fig. 2, the protons adsorbed by the Al-PILC supports as a function of the precursor solution pH, can be observed in Fig. 2. Accordingly, the acidity values, measured by ammonia adsorption, are directly related to the pH of the starting solution, as shown in Table 3.

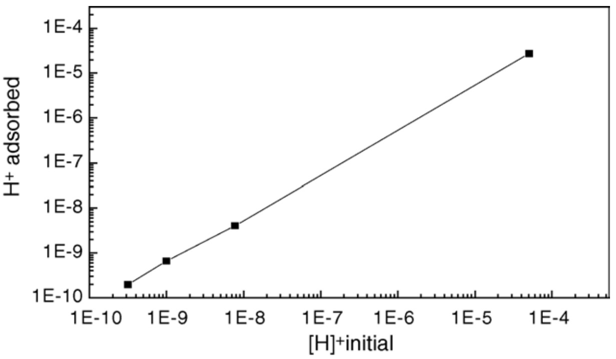

Fig. 2. Influence of the impregnating solution initial pH on the adsorbed protons during Pd incorporation on monolithic supports.

Likewise, metallic dispersion can be explained as a consequence of these parameters: when the difference between the impregnating solution pH and the solution IEP is high, the bonding strength between the incorporated cationic metallic phase and the support surface is also high and the metal will be well dispersed and stable; the contrary holds when the difference is small. Thus, high pH values will give rise to high dispersion and low pH to lower dispersion, as shown in Table 3.

Catalyst C23 synthesized at pH 9.5 had the highest metal dispersion and lowest acidity of the series. In contrast, sample C12 synthesized at the lowest pH among those obtained from ammonia solution had the lowest metallic dispersion but the highest acidity. Sample C13 from a solution with an intermediate pH had intermediate values of dispersion and acidity. For sample C25, prepared at a pH resulting from the direct aqueous solution of palladium acetate, proton incorporation was high. However, the corresponding Pd cationic species was only slightly adsorbed on the support surface, resulting in the highest acidity but low metallic dispersion.

A large difference between the impregnating solution pH and the IEP results in rapid cationic adsorption on the external surface of the solid, making solute diffusion difficult within the clay interlayer. On the contrary, when the difference is small, slower adsorption takes place, as the metal gradient in the penetrating solution is almost non-existent and Pd ions diffuse into the interlayer, reaching positions close to or over the Al pillars.

Table 4 shows the binding energies for the predominant elements in the samples, Si, Al and Pd, in addition to the surface atomic ratios measured by XPS on some of the

Table 3
Main physico-chemical properties of the studied catalysts

Catalyst	d_{001} (Å)	V_{micro} ($cm^3 g^{-1}$)	V_{meso} ($cm^3 g^{-1}$)	V_{macro} ($cm^3 g^{-1}$)	V_{total} ($cm^3 g^{-1}$)	S_{BET} ($m^2 g^{-1}$)	Acidity (meq g^{-1})	Dispersion (%)
M500	18.2	0.045	0.083	0.202	0.330	217	1.42	–
C25	18.2	0.038	0.075	0.215	0.328	193	1.48	30
C12	18.2	0.041	0.066	0.213	0.320	193	1.41	25
C13	18.2	0.044	0.076	0.218	0.338	214	1.37	50
C23	18.2	0.041	0.080	0.220	0.341	197	1.36	93

Table 4
XPS binding energy (eV) and surface atomic ratio of the main elements

Catalyst	Al 2p	Si 2p	Pd $3d_{5/2}$	Si/Al
C12	74.3	103.2	337.8	2.63
C13	74.2	102.9	337.7	2.18
C23	74.2	102.9	337.7	1.07

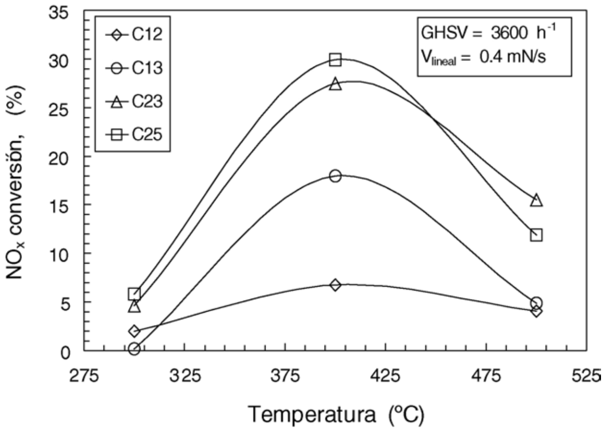

Fig. 3. Influence of operating temperature on nitric oxide molar conversion on the Pd/ Al-PILC monolithic catalysts.

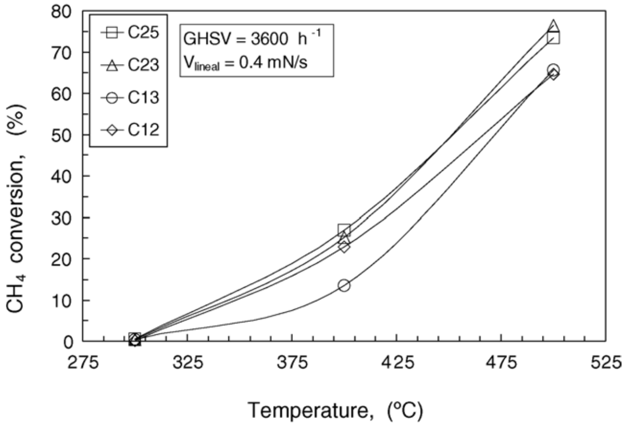

Fig. 4. Influence of operating temperature on methane conversion on the Pd/Al-PILC monolithic catalysts.

samples. It can be observed that palladium is in the form Pd^{2+} in all the samples and that Pd ions must be surrounded by electronegative ions, especially for sample C12, because its binding energy (337.8 eV) is slightly higher than that for homologs in the series. The Si/Al atomic ratio measured indicates that Pd in sample C12, impregnated at low pH, was deposited mainly over Al, whereas deposition in sample C23 was over Si and C13 was intermediate between these. Given the aforementioned differences, adsorption should be quicker at high pH and the metal should deposit on the exposed surface silicon atoms. In contrast, at lower pH, adsorption is slower and Pd can diffuse into the interlayer space and reach positions over aluminum, either from the edges or from the pillars.

Molar conversions of NO and CH_4 versus temperature over all the catalysts are shown in Figs. 3 and 4, respectively. No N_2O formation was observed for any of the catalysts. It can be observed that NO conversion exhibited a volcano curve with increasing temperature, typical for reactions in which two reactants with different activation energy (NO and O_2) compete for another one (CH_4). The activation energy for methane reaction with O_2 (combustion) is higher than for NO; thus, above a certain temperature, in this case 400 °C, the former reaction dominates the process. The results at the optimum reaction temperature, 400 °C, are shown in Table 5. C25 synthesized at the lowest pH and from acetate solution gave the best NO molar conversion of the series.

The catalytic activity cannot be directly related to the textural properties, Pd content or dispersion, or the acidity, but rather a combination of all of these, which in turn is strongly related to the preparation method. According to the literature, NO_x reduction with hydrocarbons (ethylene) in oxygen excess for Cu^{2+} ion-exchanged Al-PILC is due to a "unique combination" of the Cu^{2+} redox properties and the strong Lewis acidity of the pillared clay [18]. Thus, both the Cu^{2+} ion redox property and the acidity are important for the overall activity. Apparently, the acidic centers activate the hydrocarbon in the presence of oxygen to form oxygenated species, which further react with the adjacent previously chemisorbed NO_2 or NO_3^- to form nitrogen-containing hydrocarbon-oxygenated intermediates on the conjugated Al–O–Cu sites. The same mechanism has been adopted in reduction by CH_4 [4]. With respect to Pd catalysts, Chin et al. [37] concluded that only Pd^{2+} was active in NO conversion, while PdO clusters mainly gave rise to methane combustion. The acid sites of the support stabilize Pd as isolated ions [38], whereas non-acidic materials lead to PdO cluster formation. Thus, both Pd dispersion and acid sites are necessary to achieve high $DeNO_x$ activity and selectivity.

During the Pd impregnation step, exchange can occur between the exchangeable support cations and the metal in

Table 5
Percent conversions at 400 °C

Catalyst	X_{NO} (%)	$X_{CH_4\,total}$ (%)	$X_{CH_4\,(NO)}$ (%)	$X_{CH_4\,(O_2)}$ (%)	$X_{CH_4\,(NO)}/X_{CH_4\,total}$ (%)
C25	29.94	26.92	1.42	25.50	0.05
C12	6.74	22.83	0.31	22.51	0.01
C13	17.98	13.46	0.79	12.64	0.06
C23	27.52	25.16	1.31	23.84	0.05

Operating conditions: GHSV = 3600 h^{-1} N.C., linear velocity = 0.4 mN s^{-1}, $[CH_4]/[NO] = 10$, $O_2 = 1.2$ vol.%.

solution, provided it is in a cationic phase, such as occurred in sample C25. In this case, the main part of the metallic charge becomes structural and should remain in an ionic state in the support, even after calcination at 500 °C, thus easing NO activation. Based on the aforementioned mechanism, this last fact altogether with the high acidity of the catalyst, could explain the higher activity of C25 as compared to the rest of the series for both NO_x conversion and CH_4 combustion. For the other catalysts, such an exchange could only occur at the surface of the clay because the metallic complexes in solution could not readily penetrate the interlayer space due to their size. Thus, PdO rather than Pd^{2+} must be formed after calcination, and thus lower activity is expected. No beneficial effect of Pd within the porous system would be found for catalysts in which Pd is on the outer surface, leading to low activity.

Also, the precursor nature can play an important role in catalyst activity. Thus, for the catalysts from acetate precursors, no anionic species remain after high-temperature calcination, and thus Pd activity should be related only to metal dispersion and acidity. However, when palladium chloride is the precursor salt and the corresponding ammine complexes were formed after aqueous ammonia addition, the coordination sphere of the cation may not be completed by ammonia. In this case additional bonding with the chloride anion still in solution could occur, remaining on the solid surface after calcination. As a result, Pd should be in a more polarized environment, shown by the higher binding energy detected by XPS, and the activity for NO_x reduction is lower, although there were effects on methane combustion.

4. Conclusions

The preparation of Al-PILCs in concentrated acetone suspension (50% clay) was a convenient method for the industrial preparation of good-quality Al-based PILCs. The materials were successfully applied, after suitable addition of the parent material as permanent binder, to the preparation of structured materials for use as monolithic catalyst supports, without any appreciable loss of the physico-chemical properties of the forming material. High surface area, low density and high mechanical strength, together with proven thermal and chemical stability, were shown by these monoliths, which make them a valuable alternative for NO_x SCR with methane in oxygen excess and generally in any process in which large gas volumes are involved.

Impregnation of these monolithic supports to form Pd catalysts follows the same tendency as any other catalyst preparation process: direct dependence on the solution pH in relation to the IEP of the solid and on speciation of the palladium complexes in solution. Properties such as acidity, metallic dispersion and location of the active phase, all of which influence the activity and selectivity of the final catalyst, are strongly dependent on the pH. Knowledge of this dependence should facilitate the prediction of catalyst performance and, inversely, help in selecting optimum conditions for the impregnation step.

Acknowledgements

The authors gratefully acknowledge the Madrid Community for financial support of this work under Project CAM 07M/0119/2000. We also thank Prof. Jose Luis Garcia Fierro for the XPS spectra and fruitful discussions on the theme.

References

[1] J.N. Armor, Catal. Today 26 (1995) 147.
[2] A. Bahamonde, S. Campuzano, M. Yates, P. Salerno, S. Mendioroz, Appl. Catal. B: Environ. 44 (2003) 333.
[3] Y. Li, J.N. Armor, Appl. Catal. B: Environ. 2 (1993) 239.
[4] V.I. Parvulescu, P. Grange, B. Delmon, Catal. Today 46 (1998) 233.
[5] M.D. Fokema, J.Y. Ying, Catal. Rev. 43 (2001) 1.
[6] R.T. Yang, N. Tharappiwattananon, R.Q. Long, Appl. Catal. B: Environ. 19 (1998) 289.
[7] A. Gil, L.M. Gandia, M.A. Vicente, Catal. Rev. Sci. Eng. 42 (2000) 145.
[8] J.T. Klopproge, W.J.J. Walters, E. Booy, V.H.J. de Beer, R.A. van Santen, J.W. Geus, J.B.H. Janssen, Appl. Catal. A: Gen. 97 (1993) 77.
[9] J.G. Pacheco, J.A. de los Reyes, G.A. Fuentes, Proceedings of the 16th Simposio Iberoamericano Catálisis, Bucaramanga (Colombia), 1998, p. 55.
[10] P. Salerno, S. Mendioroz, A. Lopez Agudo, Appl. Catal. A: Gen. 259 (2004) 17.
[11] R. Ramos, A. Lopez, M.J. Martinez, S. Robles, A. Castillo, G. Sandoval, J.M. Domínguez, Proceedings of the 16th Simposio Iberoamericano Catálisis, Bucaramanga (Colombia), 1998, p. 337.
[12] J. Monnier, J.P. Charland, J.R. Brown, M.F. Wilson, Stud. Surf. Sci. Catal. 75 (1993) 1943.
[13] D.E.W. Vaughan, Catal. Today 2 (1988) 187.
[14] C. Philippopoulos, N. Gangas, N.J. Papayannakos, J. Mater. Sci. Lett. 15 (1996) 1940.
[15] S. Morfis, C. Philippopoulos, N.J. Papayannakos, Appl. Clay Sci. 13 (1998) 203.
[16] L.S. Cheng, R.T. Yang, N. Chen, J. Catal. 164 (1996) 70.
[17] R.Q. Long, R.T. Yang, Catal. Lett. 59 (1999) 39.
[18] W. Li, M. Sirilumpen, R.T. Yang, Appl. Catal. B: Environ. 11 (1997) 347.
[19] A. Cybulski, J.A. Moulijn, Structured Catalysis and Reactors, Marcel Dekker, Inc., New York, 1998.
[20] S. Irandoust, B. Andersson, Catal. Rev. Sci. Eng. 30 (3) (1988) 341.
[21] P. Forzatti, Catal. Today 62 (2000) 51.
[22] G. Groppi, W. Ibashi, E. Tronconi, P. Forzatti, Catal. Today 69 (1–4) (2001) 399.
[23] I.W. Lachman, J.L. Williams, Catal. Today 14 (1992) 317.
[24] S. Lee, R. Aris, Catal. Rev. Sci. Eng. 27 (2) (1985) 207.
[25] C. Marcilly, J.P. Franck, Revue de l'Ìnstitute Français du Pétrole 39 (3) (1984) 337.
[26] K. Morikawa, T. Shirasaki, M. Okada, Adv. Catal. 20 (1969) 97.
[27] B.N. Shelimov, J.F. Lambert, M. Che, B. Didillon, J. Mol. Catal. A: Chem. 158 (2000) 91.
[28] W.A. Spieker, J.R. Regalbuto, Chem. Eng. Sci. 56 (2001) 3491.
[29] W.A. Spieker, J. Liu, X. Hao, J.T. Miller, A.J. Kropf, J.R. Regalbuto, Appl. Catal. A: Gen. 243 (2003) 53.
[30] J.P. Brunelle, Pure Appl. Chem. 50 (1978) 1211.

[31] C. Contescu, M.I. Vass, Appl. Catal. 33 (1987) 259.
[32] P. Salerno, S. Mendioroz, Appl. Clay Sci. 22 (2002) 115.
[33] F. Mohino, A.B. Martin, P. Salerno, A. Bahamonde, S. Mendioroz, Appl. Clay Sci. 29 (2) (2005) 125.
[34] R.M. Heck, R.J. Farrauto, S.T. Gulati, Catalytic Air Pollution Control Commercial Technology, 2nd ed., John Wiley and Sons, Inc., New York, 2002.
[35] A. Molinard, PhD thesis, Antwerpen, 1994.
[36] J.R. Regalbuto, M. Schrier, X. Hao, W.A. Spieker, J.G. Kim, J.T. Miller, A.J. Kropf, Stud. Surf. Sci. Catal. 143 (2002) 45.
[37] Y.H. Chin, W.E. Alvarez, D.E. Resasco, Catal. Today 62 (2000) 291.
[38] Y.H. Chin, A. Pisanu, L. Serventi, W.E. Alvarez, D.E. Resasco, Catal. Today 54 (1999) 419.